TU Delft

Delft University of Technology

Document Version
Final published version

Licence
CC BY

Citation (APA)
Kortenbout, A. J., Camfferman, F. A., Kagenaar, W., Govaert, P., Alderliesten, T., Tataranno, M. L., de Jong, N., Vos, H. J., Bosch, J. G., & More Authors (2026). Cerebral High-Frame-Rate Ultrasound Imaging and Its Possibilities in the Neonatal Intensive Care Unit. *Ultrasound in Medicine and Biology*, *52*(11), 2458-2467. https://doi.org/10.1016/j.ultrasmedbio.2026.07.009

Important note
To cite this publication, please use the final published version (if applicable).
Please check the document version above.

Copyright
In case the licence states “Dutch Copyright Act (Article 25fa)”, this publication was made available Green Open Access via the TU Delft Institutional Repository pursuant to Dutch Copyright Act (Article 25fa, the Taverne amendment). This provision does not affect copyright ownership.
Unless copyright is transferred by contract or statute, it remains with the copyright holder.

Sharing and reuse
Other than for strictly personal use, it is not permitted to download, forward or distribute the text or part of it, without the consent of the author(s) and/or copyright holder(s), unless the work is under an open content license such as Creative Commons.

Takedown policy
Please contact us and provide details if you believe this document breaches copyrights.
We will remove access to the work immediately and investigate your claim.

This work is downloaded from Delft University of Technology.

Ultrasound in Medicine & Biology 52 (2026) 2458–2467

Contents lists available at ScienceDirect

Ultrasound in Medicine & Biology

journal homepage: www.elsevier.com/locate/ultrasmedbio

Original Contribution

Cerebral High-Frame-Rate Ultrasound Imaging and Its Possibilities in the Neonatal Intensive Care Unit

Anna J. Kortenbout [a], Fleur A. Camfferman [b], Wieke Kagenaar [c], Paul Govaert [d], Thomas Alderliesten [c], Maria Luisa Tataranno [c], Manon Benders [c], Nico de Jong [a,e], Hendrik J. Vos [a,e], Johan G. Bosch [a], Jeroen Dudink [c,*]

[a] Department of Cardiology, Thorax Biomedical Engineering, Erasmus MC University Medical Centre, Rotterdam, The Netherlands
[b] Department of Neonatology, Universitair Ziekenhuis Brussel, VUB, Brussels, Belgium
[c] Department of Neonatology, Wilhelmina Children's Hospital, University Medical Centre Utrecht, Utrecht, The Netherlands
[d] Department of Neonatology, ZNA Middelheim, Antwerp, Belgium
[e] Faculty of Applied Sciences, Department of Imaging Physics, Delft University of Technology, Medical Imaging, Delft, The Netherlands

ARTICLE INFO

Keywords:
High frame rate
Cerebral Doppler ultrasound
Neonates
Resistivity index
Blood flow

ABSTRACT

Objective: Impaired cerebral blood flow in preterm neonates is a risk factor for developing brain injury. High-frame-rate (HFR) ultrasound (US) imaging using plane-wave transmissions enables spectral Doppler-based flow analysis in all imaging pixels with high spatiotemporal resolution and sensitivity, potentially providing a better indicator of neonatal cerebral blood flow. The aim was to investigate the feasibility of HFR US in measuring cerebral blood flow velocities in the periventricular zone of newborn infants. Secondary aims: (i) differentiate between venous and arterial flow, (ii) investigate the impact of unilateral brain injury on blood flow and (iii) examine the influence of patient variables on HFR results.

Methods: In a prospective cohort study, 2-D HFR US imaging data in (pre)term infants were recorded with a custom HFR mode on a Zonare ZS3 system with a high-frequency linear probe (L20-5). Data were analyzed offline to calculate peak systolic velocity (PSV), end diastolic velocity, resistivity index and the new flow index (FI), defined as the average PSV across all blood flow pixels within a region of interest.

Results: HFR US was performed in 81 patients (118 HFR recordings) of which 72 recordings were excluded due to technical limitations or insufficient image quality. In the remaining 46 recordings, arterial and venous flow could be reliably distinguished. In neonates with unilateral intracranial pathology ($n = 12$), the median FI was higher on the affected side (1.62, IQR 1.48–1.79) compared to the contralateral side (1.41, IQR 1.33–1.50; $p = 0.002$). Across all recordings, FI showed no significant correlation with birth weight ($\rho = 0.11$, $p = 0.42$), post-menstrual age ($\rho = 0.07$, $p = 0.56$), z-scores or mean airway pressure in ventilated infants.

Conclusion: Obtaining qualitative and quantitative flow indices with HFR US imaging is feasible in a population of neonates. HFR-derived perfusion indices may play an important role in understanding and preventing neonatal brain injury.

Background

Preterm neonates have a high risk of developing brain injury [1,2]. Maintenance of adequate blood flow and oxygenation to meet metabolic demand in the brain is crucial to normal brain development [3]. It can prevent injury and mortality associated with severe brain damage [4,5].

However, monitoring cerebral perfusion is challenging, especially in the typically unstable preterm neonate. Near-infrared spectroscopy (NIRS) enables continuous, bedside monitoring of regional cerebral oxygen saturation and provides insight into the balance between cerebral oxygen delivery and consumption. NIRS is widely used in neonates for monitoring cerebral oxygenation, assessing cerebral autoregulation and neurovascular coupling. However, NIRS does not provide a quantitative measurement of cerebral blood flow and lacks spatial localization due to its limited penetration depth and large sampling volume [6]. A quantitative, safe and bedside method for measuring cerebral blood flow is still lacking.

Cranial ultrasound (CUS) is widely used for the evaluation of neonatal brain anatomy and detection of brain injury, since it is non-invasive and harmless [7]. It is less expensive than other imaging methods, can

* Corresponding author. Department of Neonatology, Wilhelmina Children's Hospital, University Medical Center Utrecht, Lundlaan 6, 3585EA Utrecht, The Netherlands.
E-mail address: j.dudink@umcutrecht.nl (J. Dudink).

https://doi.org/10.1016/j.ultrasmedbio.2026.07.009
Received 17 December 2025; Revised 29 June 2026; Accepted 14 July 2026

0301-5629/© 2026 The Authors. Published by Elsevier Inc. on behalf of World Federation for Ultrasound in Medicine and Biology. This is an open access article under the CC BY license (http://creativecommons.org/licenses/by/4.0/)

be performed bedside with minimal discomfort to the baby, and allows for repeated examinations. This enables frequent scanning to monitor abnormalities over time and facilitates the tracking of physiological processes [8–10]. Furthermore, ultrasound (US) is not limited by the shallow penetration depth of optical techniques such as NIRS and can therefore be used to assess deeper-lying brain structures and cerebral vasculature.

Conventional color Doppler US allows qualitative visualization of vessels with mean blood flow velocities in 2-D. In spectral Doppler mode, a blood flow velocity spectrum can be measured. This allows for quantification of the velocity by tracing the envelope of this spectrum and extracting peak systolic velocity (PSV), end-diastolic velocity (EDV), resistivity index (RI) and pulsatility index (PI) [11]. However, flow indices like RI and PI, which were historically used as a proxy for vascular autoregulation and intracranial hypertension [12–14], do not appear to predict brain injury or long-term neurodevelopmental outcome in preterm infants [15].

A major limitation of conventional Doppler US is its low frame rate, which restricts it either to provide a qualitative 2-D map of vessels using color Doppler or to provide a quantitative measurement in a single artery or vein using spectral Doppler. High-frame-rate (HFR) US imaging, capable of reaching frame rates up to 10,000 frames per second, addresses this limitation [16]. This technique uses plane or diverging wave transmissions covering the entire field of view at once, as opposed to the traditional beam-by-beam line scan method of conventional Doppler US. The high frame rate facilitates more effective filtering, enhancing the distinction between slowly moving tissue and blood flow in slow-flow vessels [16]. Additionally, HFR imaging allows for comprehensive analysis of the temporal profile across an entire cardiac cycle within the vessels in the entire field of view. Consequently, this technology enables the generation of images characterized by both high spatiotemporal resolution and increased sensitivity to blood flow [17], facilitating the investigation of alterations in blood flow resulting from or possibly even preceding brain injury.

In adults, this technique has already been used in cardiac [18,19], carotid [20,21] and ocular studies [22]. HFR cerebral US has also shown promising results in small studies in neonates [13,23], where it is more sensitive to smaller blood vessels. However, there are no data in larger cohorts of (pre)term infants. Currently, no universally accepted gold-standard method exists for arterial-venous differentiation in neonatal HFR US imaging. Previous studies have used combinations of anatomical vessel identification, blood-flow directionality, physiological flow characteristics and expert assessment as reference standards for validation of automated classification methods [24,25]. These studies highlight the potential of HFR US for vessel characterization. In the present study, we adopted a similar validation strategy while exploring a simplified physiologically based classification approach aimed at routine bedside implementation. This study focuses on the clinical feasibility of bedside HFR US imaging using a conventional clinical scanner in a cohort of preterm neonates. Differentiating between arterial perfusion and venous drainage may improve understanding of neonatal cerebral hemodynamics, particularly because disturbances in both arterial inflow and venous outflow have been associated with the pathophysiology of several preterm brain injury patterns, including intra-ventricular hemorrhage (IVH), venous infarction and white matter injury [26]. US localization microscopy is another emerging technique for microvascular imaging that may employ HFR techniques; however, it requires intravenous microbubble contrast administration and prolonged acquisition times, which currently limit its routine bedside applicability in neonates [27].

This study aimed to measure cerebral blood flow velocities in neonates' periventricular zone using HFR Doppler imaging, with secondary objectives: (1) to differentiate between venous and arterial flow (2), to investigate the impact of brain injury on periventricular blood flow and (3) to evaluate the association between clinical and maturational variables, including birth weight, post-menstrual age, post-natal age and mean arterial blood pressure, and Doppler-derived hemodynamic parameters, specifically PSV, EDV and resistive index, obtained using spectral Doppler analysis applied to HFR US imaging data.

Methods

Study design

All infants admitted to our neonatal intensive care unit (NICU) from July 2019 to March 2022 were eligible for inclusion in the study. Parental informed consent was obtained whenever a trained operator in the HFR CUS protocol was available. Exclusion criteria were: major language barrier and clinical instability as judged by the attending physician.

This prospective study was reviewed by the institutional ethics committee and classified as an observational cohort study under the applicable national regulatory framework.

All US examinations were performed as part of routine CUS monitoring according to standard clinical care. The only study-related addition consisted of a single HFR acquisition obtained during the same examination. This additional acquisition was performed without extra handling, sedation or administration of contrast agents and therefore represented minimal additional burden for the infant.

Written informed parental consent was obtained from the parents or legal guardians of all included infants prior to participation.

Data collection

Clinical variables were collected prospectively and predefined prior to analysis. These included maturational variables (birth weight, gestational age (GA), post-menstrual age at time of scanning and weight z-score), respiratory support variables (requirement for mechanical ventilation and mean airway pressure [MAP]) and neurological variables (presence and lateralization of intracranial pathology as determined by routine CUS).

These variables were selected because of their potential influence on cerebral hemodynamics, vascular maturation and Doppler-derived flow parameters. Ventilator settings, relevant medical diagnoses and relevant findings on clinical US scans were extracted from the patients record.

In included infants, routine CUS was performed at recommended moments [28] using a Zonare ZS3 US machine (Mindray Medical International, San Jose, CA, USA). After completion of the routine examination, a high-frequency linear probe (L20-5, center frequency 11 MHz) was positioned to obtain a symmetric coronal imaging plane at the level of the interventricular foramen. The transducer was manually positioned on the anterior fontanelle according to standard neonatal CUS practice, using sterile water-soluble US gel for acoustic coupling and without additional fixation devices. Probe positioning was standardized using the frontal horns of the lateral ventricles and the cavum septi pellucidi as additional anatomical landmarks to confirm midline alignment and symmetry. After confirmation of the imaging plane, the system was switched to the custom HFR acquisition mode as described previously [29]. HFR acquisition was performed on the CE-marked Zonare ZS3 US platform using a manufacturer-provided research implementation. This research mode enabled access to beamformed IQ data and modified acquisition parameters not available in the standard clinical software, while operating within approved safety limits (MI below 0.1). It was used exclusively for data acquisition and offline analysis and did not influence clinical decision-making.

A custom plane-wave–type transmission sequence without angular compounding was applied. Depending on the software version, the effective acquisition frame rate was 650 or 1050 Hz, corresponding directly to the pulse repetition frequency of the Doppler sequence. For each recording, 2000 frames were acquired and stored for offline analysis. Further technical details have been described previously [29]. If an infant had multiple routine CUS exams during their NICU stay, multiple HFR measurements were attempted. HFR measurements were included

if adequate signal was present in the periventricular zone and no significant motion artifacts were present. Recordings were included based on visual assessment confirming the presence of detectable flow signals within periventricular vessels suitable for subsequent signal analysis. No dedicated motion correction algorithm was applied. Recordings with visible motion artefacts were partially excluded during offline processing (up to 1000 frames), and analysis required at least two complete cardiac cycles to ensure reliable velocity estimation.

Outcome measures and data analysis

HFR images were analyzed offline using in-house developed scripts written in MATLAB (MathWorks MATLAB [R2022a], Natick, MA, USA). Clutter filtering was performed using a singular value decomposition (SVD) based spatiotemporal filtering approach. The original IQ data were smoothed using a spatiotemporal Gaussian filter with a $3 \times 3 \times 3$ kernel size (axial × lateral × temporal) to reduce noise prior to SVD filtering. A low-rank threshold selection algorithm was applied to determine the cut-off between tissue and blood-flow–related SVD components, in accordance with established HFR US imaging filtering methods [30,31]. The threshold was determined automatically for each acquisition based on its singular value spectrum, and no fixed SVD rank was predefined for recordings acquired at 650 or 1050 Hz. Minor variations in rank selection primarily affected components near the clutter–flow boundary and did not result in systematic changes in detected vascular structures or regional flow index (FI) values. Illustrative examples of a spatial correlation matrix and power Doppler images obtained with varying SVD thresholds are provided in the Supplementary Material [30]. Next, a spectrogram for each valid blood flow pixel over time was calculated. These spectrograms were further processed with an automatic maximum likelihood envelope detection algorithm, described in our previous paper [29], representing local blood flow velocity at each timepoint. This velocity tracing allowed for pixel-wise calculation of blood flow parameters, such as PSV, EDV and RI. PSV and EDV in cm/s were calculated by averaging minima and maxima of the envelope per heartbeat over all heartbeats [29]. RI was calculated by $RI = \frac{PSV-EDV}{PSV}$. Quantitative parameter maps were created for all blood flow pixels and further analyzed in both hemispheres. To ensure left-right comparability, in each recording an oval region of interest (ROI) of identical dimensions was manually selected in the power Doppler image at approximately the same depth in both hemispheres. The ROIs were selected to maximize the inclusion of valid blood flow pixels, while excluding areas with higher noise levels. ROIs were selected with comparable size across recordings by a single trained observer. The analysis focused on intra-parenchymal and periventricular vessels within the white matter and did not target extra-parenchymal venous sinuses.

With the quantitative information on each blood vessel in the ROI, we developed a new index as representative for cerebral blood flow per hemisphere: the FI. This FI was calculated by $FI = \frac{\sum PSV \text{ of blood flow pixels}}{\text{Total number of blood flow pixels in ROI}}$ and represents average PSV for the ROI in cm/s. We also calculated a hemispheric flow difference (HFD) as a difference between FI in both hemispheres. For hemispheric analysis, bilateral ROIs were defined within the same HFR acquisition when both hemispheres were adequately visualized. Because plane-wave imaging insonifies the entire field of view simultaneously, Doppler-derived parameters from the left and right hemispheres were obtained under identical acquisition conditions without repositioning of the probe. In cases where bilateral HFR signal quality was insufficient, recordings from a single hemisphere were included for regional hemodynamic analysis only. These unilateral recordings were not used for hemispheric comparison analyses and should be interpreted as regional measurements rather than representations of global cerebral perfusion. The presence and lateralization of intracranial pathology were documented and considered during interpretation.

Classification of arteries and veins

The original frames were filtered with a Doppler wall filter (cutoff 100 Hz) in order to show the pulsation of blood flow. After that, the average time intensity over all pixels was calculated. This signal was used to automatically extract heart rate and timing of systolic peaks and end-diastolic valleys needed for testing arterial pulsatility.

To classify the spectrograms as arterial, venous or indeterminate, we applied several threshold criteria on the spectral envelope. Figure 1 shows the steps involved in an example case. The thresholds used were determined empirically based on a test set of five high-quality measurements with sufficient vessel signals in both hemispheres to allow reliable visual and anatomical classification. Directional power Doppler served as the reference for anatomical accuracy.

First, spectrograms with an average envelope level <0.2 cm/s were classified as indeterminate, as these signals often contained excessive noise.

Second, the variability of the envelope signal was assessed, as pulsating arterial signals show more variability than venous signals. We quantified this variability using the coefficient of variation (CV), calculated as $\mathrm{CV} = \frac{\text{standard deviation (envelope)}}{\text{mean (envelope)}}$.

Finally, we compared the average absolute time difference between systolic peaks in the spectrogram (Fig. 1b) with those in the general pulsatility signal (Fig. 1a).

A spectrogram was classified as arterial if it had a time difference $\leqq$8 ms and a CV $\geqq$ 0.18. Spectrograms with a CV < 0.18 were classified as venous. If the CV was $\geqq$0.18, but the time difference was > 8 ms, the spectrogram was considered indeterminate. Figure 1f shows the classification in the example case. The entire classification decision process is illustrated in Figure 2.

To validate our discrimination method, we conducted two independent validations: (1) classification based on anatomy and (2) expert manual scoring. For the anatomical classification, we classified 30 spectrograms based on their anatomical origin and flow direction. For the manual scoring, two neonatal CUS experts independently evaluated the same 30 spectrograms. As in the automatic classification, CUS experts could choose from 3 possible classifications: arterial, venous and indeterminate. We compared the anatomical classification and the expert manual scoring with our automated classification to evaluate the consistency and accuracy of our method.

Grouping

The neonates in this study were sorted into four groups based on their CUS:

1. Neonates without brain injury.
2. Neonates with unilateral brain injury (*e.g.,* IVH, perinatal arterial ischemic stroke, periventricular hemorrhagic infarction).
3. Neonates with bilateral brain injury (*e.g.,* bilateral IVH, post-hemorrhagic ventricular dilatation, bilateral punctate white matter lesions).
4. Neonates with single hemisphere recordings, regardless of the presence or absence of brain injury.

Statistical analysis

Primary outcomes were HFR US parameter maps (PSV, EDV, RI), with median values calculated within the ROIs. Secondary outcomes included correlations between HFR US parameters and clinical variables. The significance threshold was set at $p < 0.05$. Recorded patient variables were birthweight, GA, post-menstrual age, MAP (when ventilated), *z*-score and the RI of the anterior cerebral artery measured with conventional spectral Doppler.

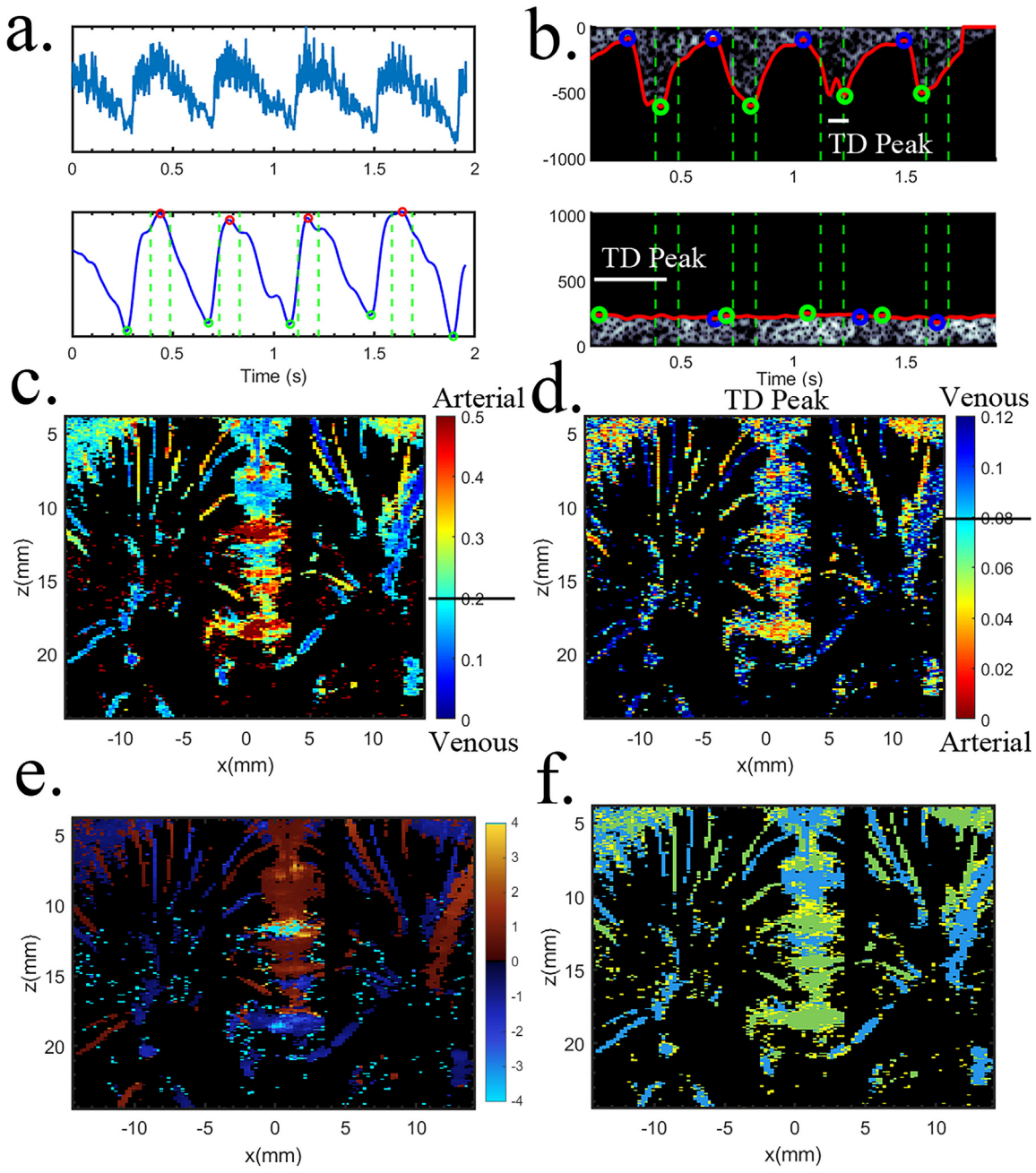


Figure 1. Illustration of the classification process in the data of a preterm neonate with IVH grade II. (a) General pulsatility signal, where red dots mark the timing of systolic peaks, and green dots identify the diastolic valleys. The green lines indicate the timing of systolic peak plus and minus 8 ms (indicative of arterial signal). (b) Two example spectrograms; the top spectrogram is an arterial signal, and the bottom one a venous signal. Green dots denote systolic peaks, while blue dots represent the end-diastolic velocity. TD is time difference in s between systolic peaks in the spectrogram and those in the general pulsatility signal. The green lines indicate the timing of systolic peak plus and minus 8 ms (indicative of arterial signal of the general pulsatility signal). (c) Map of the coefficient of variation (a.u.) across all blood flow pixels. (d) Map of TD in s. (e) Directional power Doppler with peak systolic velocity in cm/s, where red is dominant flow toward the probe and blue is flow away from the probe; the light blue pixels are either noise or aliased signals. (f) Classification of every pixel, with blue classified as venous, green as arterial and yellow as indeterminate.

The unit of analysis was the individual HFR recording. When multiple recordings per infant were available, each was analyzed independently. Hemispheric comparisons were performed only in recordings with bilateral ROIs of sufficient quality using paired analyses; recordings with unilateral ROIs were excluded from hemispheric comparisons and used only for regional analyses. Paired comparisons between hemispheres and between arterial and venous flow parameters were performed using paired t-tests.

Associations between HFR-derived parameters and clinical variables were explored using univariable linear regression analyses. Regression analyses are reported with regression coefficient and R^2.

Given the feasibility-driven nature of the study and the limited sample size, multivariable modelling was not performed. Consequently, potential collinearity between maturational variables (*e.g.*, GA, postmenstrual age, birth weight and growth indices) was not formally assessed. Correction for multiple testing was not applied, and results should therefore be interpreted as hypothesis-generating.

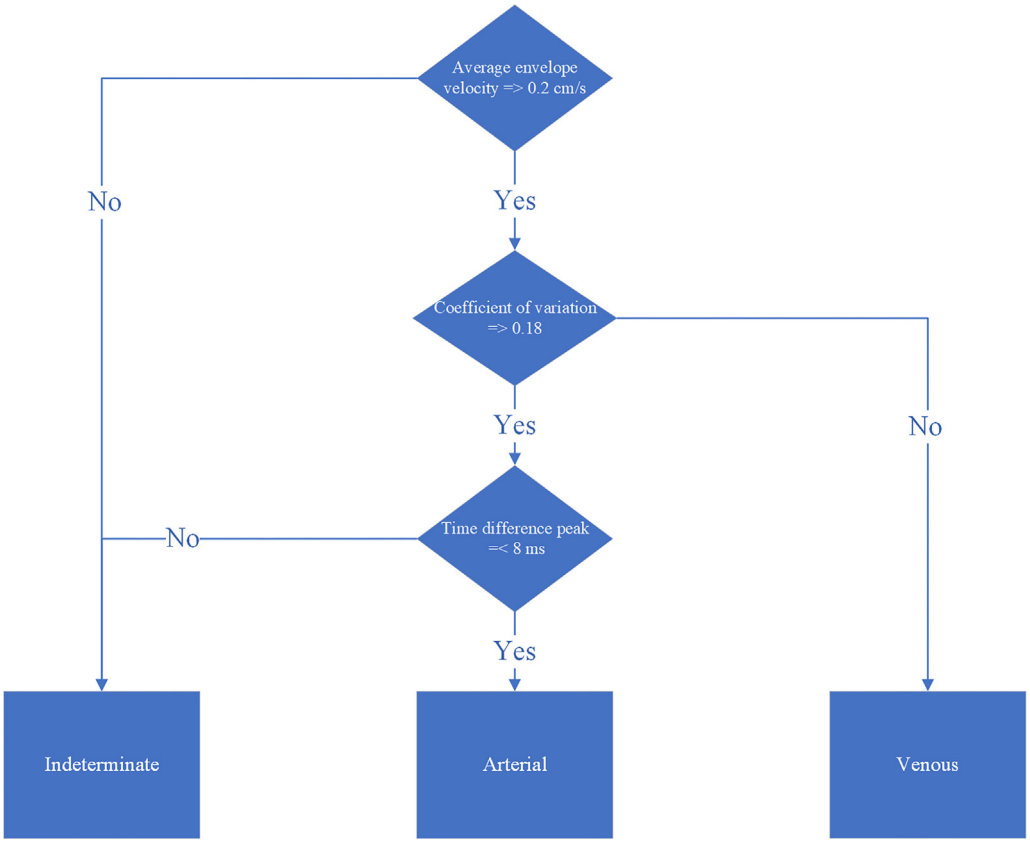


Figure 2. Decision tree of the classification process.

HFD was calculated in Group 1 (no brain injury) as left minus right FI, and in Group 2 (unilateral injury) as affected minus unaffected side. Differences were tested against zero and between groups for venous, arterial and overall flow indices.

For validation of artery and vein classification, confusion matrices compared automated results with anatomical classification and with manual scoring by two neonatal US experts (arterial, venous or indeterminate).

Results

Patient characteristics

A total of 81 patients were included in the study. Birthweight ranged from 485 to 4410 g (median 1535 g). GA ranged from 24 6/7 to 41 6/7 wk (median 30 5/7 wk). In 11 children, no HFR CUS measurement was performed due to logistic reasons (14%), 39 children had one HFR CUS recording (48%), 31 children had 2 or more recordings (38%).

During the study, 11 patients were mechanically ventilated (2 on high-frequency oscillatory ventilation). Seven patients received non-invasive positive pressure ventilation, another seven were supported with continuous positive airway pressure. The MAP was 10 (range 6–15) cm H_2O.

IVH was detected in 16 exams, periventricular hemorrhagic infarction in 4 exams, 3 patients had post-hemorrhagic ventricular dilatation, 1 patient had a perinatal arterial ischemic stroke. Mild abnormalities like lenticulostriate vasculopathy and mild periventricular echo densities were seen in 4 scans.

An inclusion chart and group division chart are given in Figure 3.

Successful US recordings

Initially, 118 HFR CUS exams were recorded. Of these, 72 HFR recordings were excluded due to technical issues (incorrect HFR settings or data-saving failures; $n_r = 14$), motion artefacts affecting image quality ($n_r = 18$) or insufficient signal quality in the periventricular zone to reliably define an ROI for analysis ($n_r = 40$). Ultimately, 46 recordings were included for further analysis. Figure 4 shows a representative measurement from a preterm neonate with IVH grade II. Figure 5 displays boxplots representing the parameter values across all groups.

Arterial/venous differentiation

Figure 6 shows the confusion matrices for the expert manual classifications and the algorithm's performance, benchmarked against the anatomical standard. These matrices illustrate the accuracy with which the experts and the algorithm identified arterial and venous blood flow. The experts achieved an inter-observer agreement of 87%, with accuracies of 87% and 93% for expert 1 and expert 2, respectively. The algorithm classified with an accuracy of 87%

Influence of patient variables

Table 1 shows the linear regression analysis of CUS parameters and patient variables. The results reveal low R^2 values (median 0.02, range 0–0.31), indicating a lack of correlation. R^2 for the RI in the ACA and the RI in the smaller periventricular arteries was 0.17, indicating a possible correlation. We also found higher R^2 values for MAP and RI in arteries ($R^2 = 0.26$) and veins ($R^2 = 0.31$). However, these findings were based on a limited subset of the population, as MAP data were available for only 17 recordings.

Hemispheric flow difference

Figure 7 presents the comparison of HFD in Group 1 (healthy neonates) and Group 2 (unilateral injury). Our findings show a significant

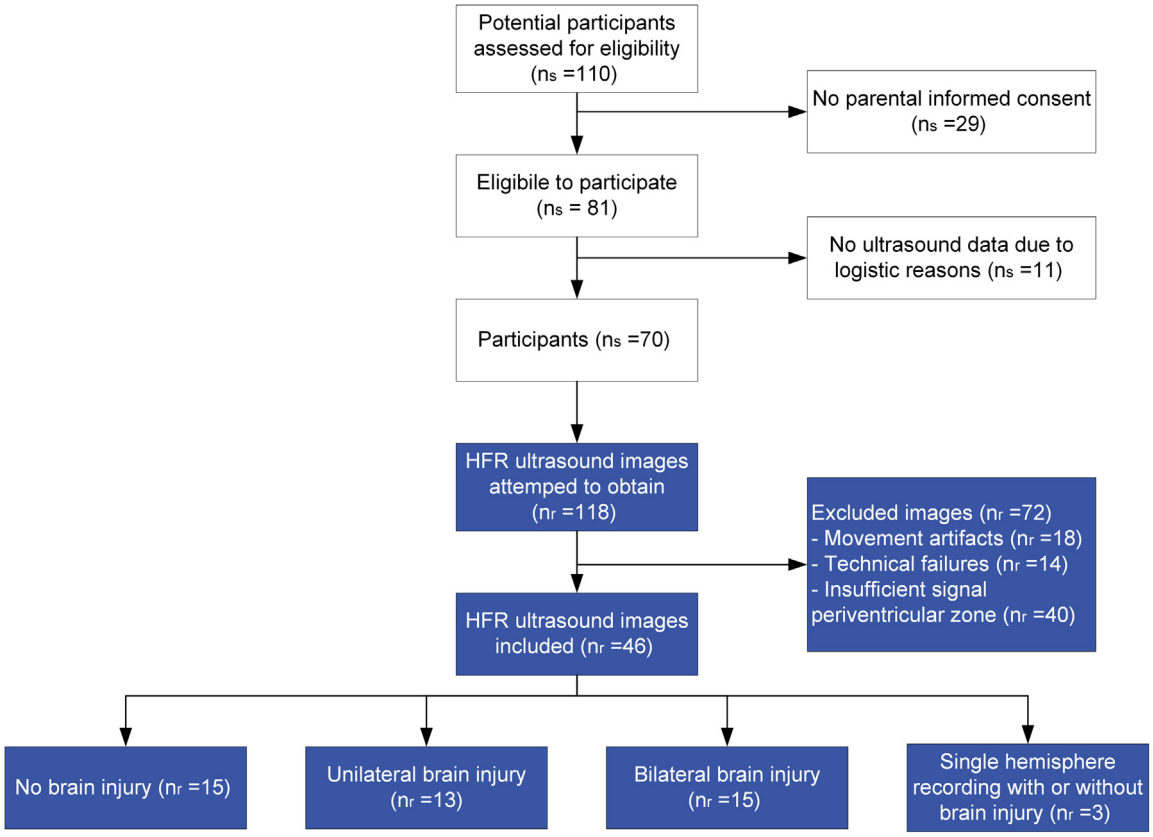


Figure 3. Inclusion chart and division chart, HFR: high-frame-rate. n_r, number of recordings; n_s, number of subjects.

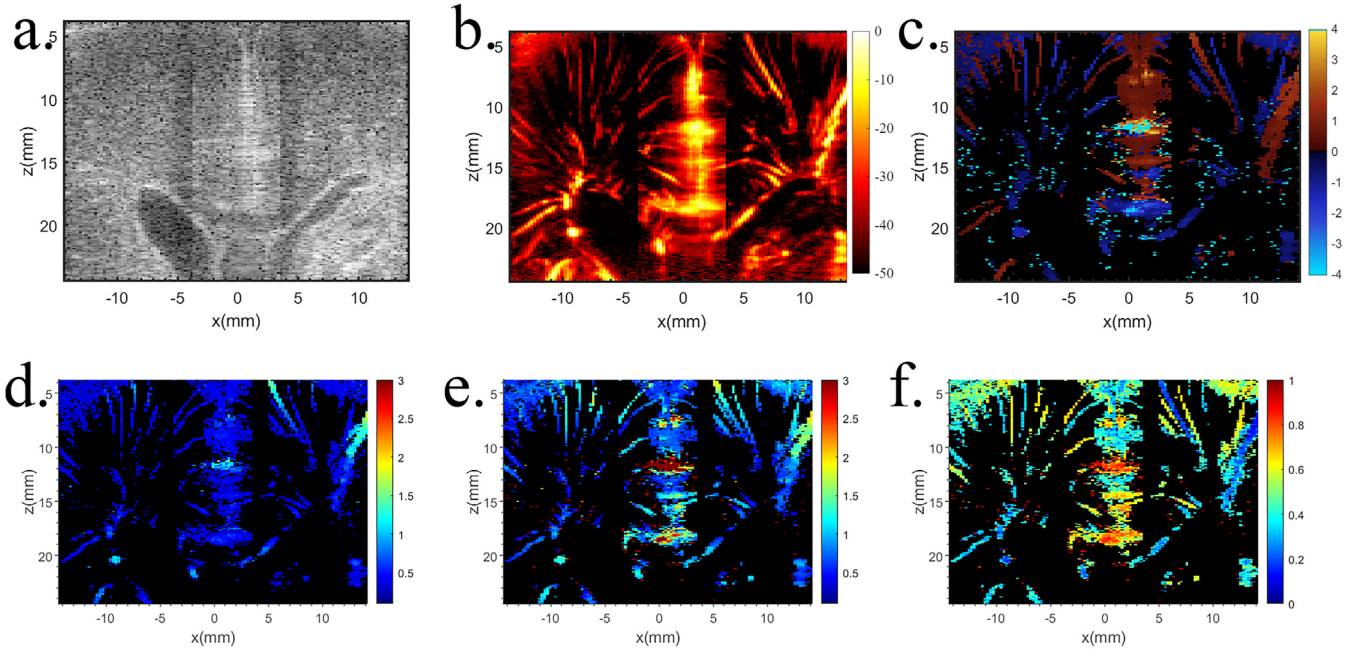


Figure 4. Measurement in a preterm neonate with an IVH in the left hemisphere. (a) Unfiltered B-mode data. (b) Power Doppler data (in dB) after smoothing and singular value decomposition filtering with ROI selection in left and right hemispheres. (c) Directional power Doppler with peak systolic velocity in cm/s; red color indicates dominant flow toward the probe and blue away from the probe; light blue pixels: noise or aliased signal. (d) Absolute end-diastolic velocity in cm/s map, (e) absolute peak-systolic velocity in cm/s map and (f) resistivity index (a.u.) map.

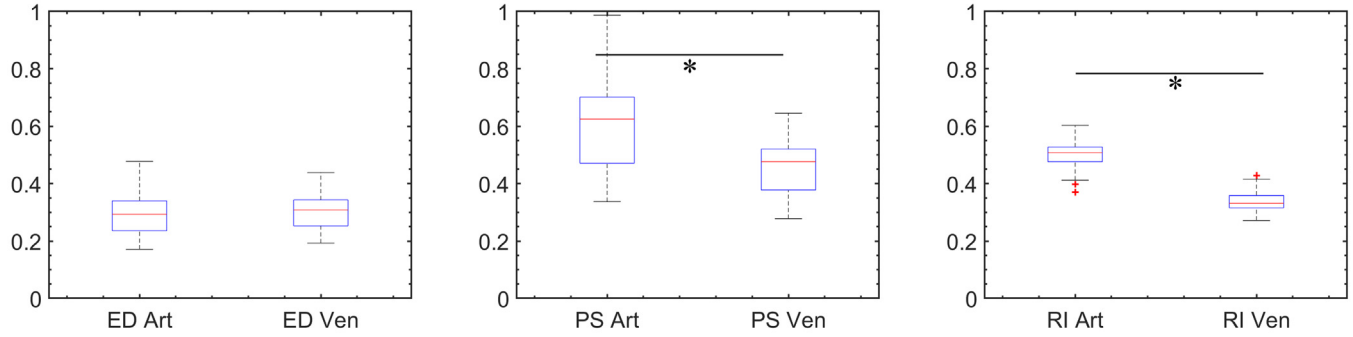


Figure 5. Boxplots of the parameter values across all groups. Art, arterial; EDV, absolute end-diastolic velocity in cm/s; PSV, absolute peak systolic velocity in cm/s; RI, resistivity index (a.u.); Ven, venous. *Indicates significance $p < 0.05$.

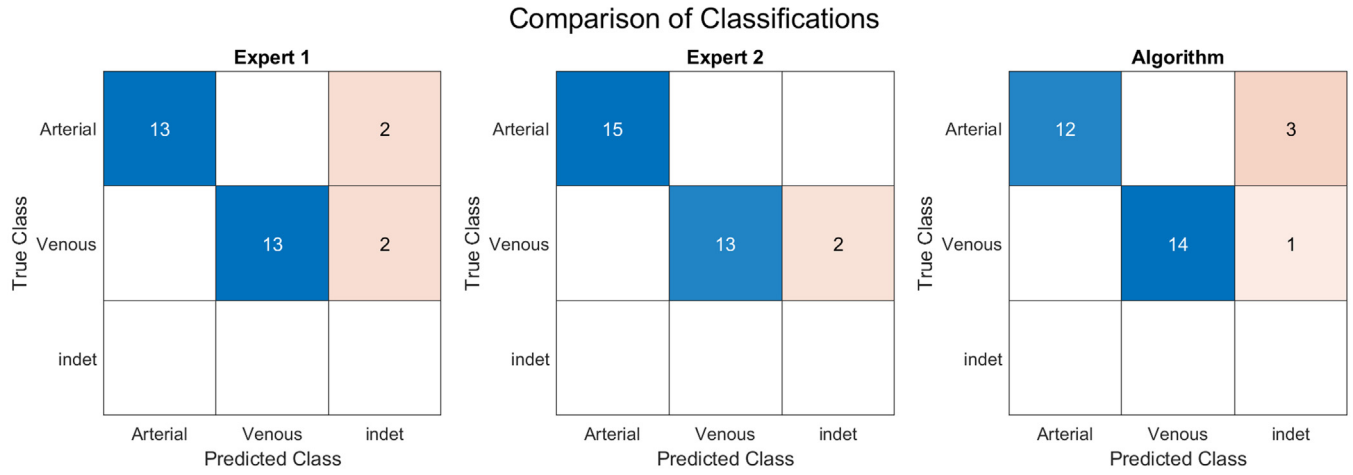


Figure 6. Comparison of classifications by 2 experts and algorithm. Indet, indeterminate.

higher FI on the affected side compared to the unaffected side. When comparing Group 2 with Group 1, there was a significant difference in the HFD of all vessels and the venous HFD, but not in the arterial HFD. The HFD in Group 3 (bilateral injury) showed no significance.

Discussion

In this study, we demonstrated that HFR CUS can provide both quantitative flow estimates and qualitative directional power Doppler information in neonates. Using this approach, arterial and venous signals were correctly distinguished in 87% of vessel segments, and in infants with unilateral brain injury, venous flow was significantly higher on the injured side. HFR-derived flow velocity results and their derived indices were independent of patient characteristics like birth weight, post-menstrual age, *z*-scores and external influences like MAP.

Table 1
Correlation (R^2) between ultrasound parameters and patient characteristics

R^2	PM	GA	BW	*z*-score	RI ACA	MAP
RI arterial	0.00	0.08	0.03	0.03	**0.17**	**0.26**
EDV arterial	0.02	0.04	0.02	0.02	0.03	0.00
PSV arterial	0.00	0.05	0.02	0.02	**0.11**	0.00
RI venous	0.02	0.01	0.00	0.00	0.10	**0.31**
EDV venous	0.00	0.08	0.08	0.08	0.00	0.00
PSV venous	0.00	**0.11**	**0.09**	**0.09**	0.01	0.01

In bold indicates that the *p* value <0.05.
BW, birthweight; EDV, end-diastolic velocity; GA, gestational age; MAP, mean airway pressure; PM, post-menstrual age; PSV, peak-systolic velocity; RI ACA, resistivity index anterior cerebral artery; RI, resistivity index.

We demonstrated that HFR CUS is accurate in discriminating between venous and arterial blood flow. This is important for enhancing our understanding of cerebral blood flow dynamics in neonates, particularly when brain injury occurs. In such contexts, significant variations between venous and arterial flow are anticipated, for instance, in venous infarction [26]. By differentiating between arterial and venous flow, we can investigate the complex interplay of arterial and venous circulation in an ROI. Our findings are in line with recent reports demonstrating the feasibility of HFR Doppler imaging for neonatal cerebral microvascular assessment and vessel differentiation [24,25]. While those studies primarily focused on technical validation and proof-of-concept implementation, the present study extends this work by evaluating HFR Doppler imaging in a clinically representative NICU cohort and assessing its feasibility in routine bedside conditions. This approach differs from recent HFR US methods that employ advanced spatiotemporal decomposition techniques (*e.g.*, ref. [32])or contrast-based flow tracking for detailed vascular mapping [33]. The present method was designed as a simplified, physiologically grounded classification strategy suitable for bedside clinical application.

Our study's results reveal a difference in the venous blood FI when comparing neonates with and without brain injury. The side of the brain injury exhibited a higher venous FI than the unaffected side. This suggests that brain injury in neonates can be associated with altered venous blood dynamics, potentially contributing to the pathophysiology of such injuries. The increased venous FI in hemispheres with focal brain injury is consistent with the known vulnerability of the immature cerebral venous system, particularly in the periventricular white matter, where disturbances in venous drainage have been implicated in the

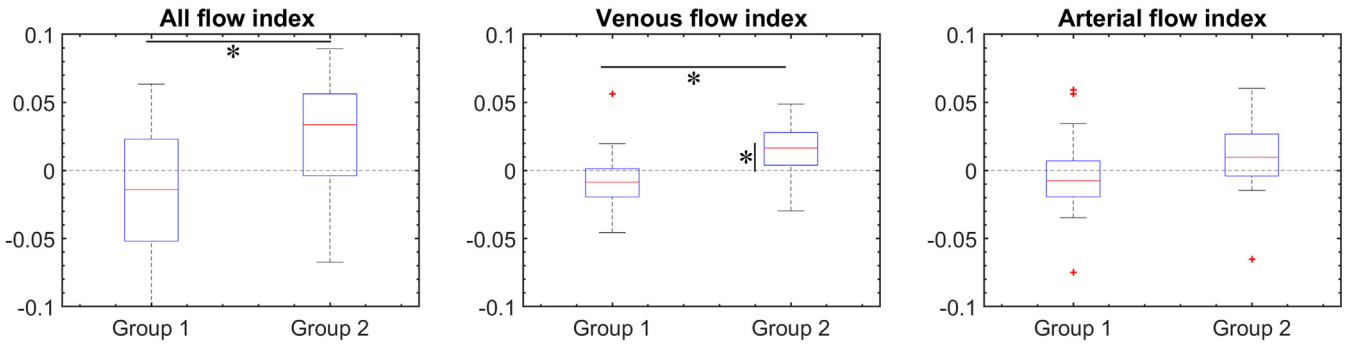


Figure 7. Hemispheric flow index difference (HFD) for all vessels, and separated for veins and arteries. Group 1 is neonates without brain injury and group 2 has neonates with unilateral brain injury. *Indicates significance $p < 0.05$.

pathogenesis of hemorrhagic infarction and white matter injury [34]. While conventional Doppler studies have mainly focused on arterial circulation, emerging data from NIRS and MRI-based perfusion imaging indicate that neonatal brain injury often reflects complex interactions between arterial inflow and venous outflow [34]. Our findings suggest that HFR US may enable regional assessment of these venous alterations. However, the cross-sectional design precludes causal inference, and longitudinal multimodal studies are needed to clarify clinical significance. Conversely, the lack of significant differences in arterial flow between the groups in our study prompts further investigation. It raises questions about the different impact of brain injuries on venous and arterial systems in neonates, a distinction that may be crucial for understanding the hemodynamic changes pre- and post-injury. If we understand this impact, we may even be able to prevent brain injury in the future.

The interpretation of regional venous hemodynamic alterations is inherently complex. Cerebral venous drainage demonstrates marked anatomical variability between individuals and between hemispheres. Variations in collateral drainage capacity and venous dominance patterns may substantially influence regional flow measurements. Additionally, extracranial factors such as head and neck position, mechanical ventilation and jugular venous compression can alter cerebral venous outflow and have been linked to the risk of germinal matrix and IVH [35,36].

Previous studies have demonstrated substantial physiological variability in cerebral venous Doppler waveforms and velocities under both normal and pathological conditions, complicating causal interpretation of observed flow changes [37]. Therefore, the increased venous flow observed in injured hemispheres in this study should be interpreted cautiously and may reflect a combination of injury-related hemodynamic alterations and underlying anatomical or systemic influences.

The FI was introduced as an exploratory summary parameter to facilitate regional and hemispheric comparison of HFR-derived blood flow velocities. FI was calculated as the average PSV across all valid blood-flow pixels within a predefined ROI and should therefore be interpreted as a regional flow velocity estimate rather than a direct measure of absolute cerebral perfusion.

FI was evaluated based on internal consistency and physiological plausibility. In neonates with unilateral intracranial pathology, FI detected significant hemispheric differences consistent with expected hemodynamic alterations, whereas no significant asymmetry was observed in infants without focal injury. These findings support the physiological sensitivity of FI but remain exploratory.

This study did not include comparison with external perfusion reference standards. Further validation in larger cohorts and against independent perfusion techniques is required.

These insights underline the clinical relevance of HFR CUS in unraveling cerebral hemodynamics. We showed that HFR CUS parameters are not significantly different when correcting for birth weight, *z*-score, post-menstrual age, post-natal age or MAP.

However, this cohort consisted of relatively stable preterm infants with largely normal MAP values and no vasoactive medication, and HFR acquisitions were only performed when infants were clinically stable enough to undergo CUS. This may limit generalizability to more critically unstable populations, in whom hemodynamic disturbances may be more pronounced.

MAP data were available only in infants receiving invasive mechanical ventilation, as MAP cannot be reliably quantified during spontaneous breathing or non-invasive support. This restricted MAP analyses to a subset of recordings and may have introduced selection bias toward more respiratory-compromised infants; correlations involving MAP should therefore be interpreted cautiously. Future studies including more hemodynamically unstable infants are needed to further evaluate clinical applicability.

A high-frequency linear probe was used for HFR Doppler acquisition. Linear probes provide higher spatial resolution and improved sensitivity for detecting low-velocity microvascular flow compared to lower-frequency sector or convex probes. This higher resolution is particularly advantageous for evaluating perfusion characteristics within superficial and periventricular brain regions, where subtle hemodynamic alterations may occur. However, the use of a high-frequency linear probe limits its penetration depth and field of view, thereby restricting assessment of deeper and more lateral cerebral structures and preventing complete organ perfusion evaluation. For this reason, the HFR recordings were performed within a predefined regional field of interest and were not intended to replace global cerebral hemodynamic assessment. All infants underwent routine CUS imaging using conventional low-frequency sector or convex probes as part of standard clinical care. The linear probe was used as a complementary research tool to obtain high-resolution HFR perfusion recordings within the selected ROI

However, there are still challenges to overcome before the HFR US can be applied in daily clinical practice. Main challenge is the sensitivity to motion of the US probe. It has to be kept still for at least 3–5 s to have a usable signal. Making sure there is always someone present to soothe the baby while the CUS exam is performed is a first step in improving the image quality. Development of a probe holder or cap is a second possibility.

Another challenge is that the frame rate was limited by the machine's software to either 650 or 1050 Hz. Theoretically, it's feasible to achieve a frame rate as high as 30 kHz with a depth range of 25 mm. Using a higher frame rate would enable the capture of a wider spectrum of velocities without the occurrence of aliasing. The current frame rate of 650 Hz was adequate for our ROI with small periventricular arteries and veins. However, this setup would not allow for the quantification of higher velocities present in larger arteries and veins.

An important limitation of our study was the relatively small proportion of measurements that met our inclusion criteria (46 successful recordings out of 118 attempts). Fourteen failed attempts were due to data-saving or acquisition-setting issues, which could likely be reduced

with further optimization of the acquisition workflow. Additionally, the current process required approximately 5 min to save each recording, limiting the possibility of repeated attempts.

Two different acquisition software versions were used during the study, resulting in frame rates of 650 or 1050 Hz. As each infant was examined with only one version, direct within-subject comparison was not possible. The use of two software versions itself represents a methodological limitation and may have introduced subtle variability in acquisition characteristics.

The present study was not powered to evaluate differences in acquisition success across GA groups. Feasibility of HFR imaging in extremely preterm infants requires further investigation in larger dedicated cohorts.

As analysis was performed offline, signal quality could not be assessed during the examination. Consequently, motion artefacts or suboptimal probe positioning went undetected at the time of acquisition, leading to the exclusion of an additional 24 measurements. These findings indicate that HFR acquisition is sensitive to motion, probe stability and operator experience, and currently demonstrates feasibility primarily under controlled bedside conditions. The current implementation represents a feasibility step toward quantitative perfusion monitoring. Translation to continuous monitoring will require automated acquisition, real-time processing and stabilized or wearable US systems. Future improvement would be to have real-time analysis of the HFR data to provide immediate quantification of cerebral blood flow in both hemispheres. Eventually, fully automated analysis would enable continuous, hands-off CUS monitoring over extended periods with compact wearable probes. Wearable single-element US devices are already being developed [38]. They provide valuable Doppler signal data across different depths, but lack the capacity to generate 2-D or even volumetric imaging information. HFR CUS, combined with a wearable probe, would be able to continuously evaluate cerebral perfusion across vessels within an entire plane.

Conclusion

Our study shows that HFR CUS imaging is a very promising technique for assessing cerebral blood flow in neonates. We demonstrated that with HFR US we are capable of differentiating between arteries and veins, independent of their orientation in the image. The unique capabilities of HFR US to provide detailed insights into both arterial and venous blood flow patterns may help us to understand and manage neonatal cerebral injury.

Despite its potential, our findings also underline the need for further research. The integration of real-time quantification will provide immediate quality control, and the expansion of evidence through larger-scale studies are important steps toward establishing HFR US as a clinically valuable tool, ultimately contributing to improved neonatal care.

Data availability statement

No consent for public data sharing is given by the participants of this study. Aggregate data may be shared upon reasonable request.

Conflict of interest

The authors declare that there are no conflicts of interest.

Acknowledgments

We thank Dr G. Mclaughlin and Dr Y. Chen of Mindray Innovation Center (San Jose, California) for the development of the custom high-frame-rate mode of the Zonare ZS3 ultrasound system. Partly funded from the project MIFFY (15293) of the OTP Research Program, financed by the Dutch Research Council (NWO).

Supplementary materials

Supplementary material associated with this article can be found in the online version at doi:10.1016/j.ultrasmedbio.2026.07.009.

References

[1] Rhee CJ, da Costa CS, Austin T, Brady KM, Czosnyka M, Lee JK. Neonatal cerebrovascular autoregulation. Pediatr Res 2018;84(5):602–10.
[2] Inder TE, Volpe JJ, Anderson PJ. Defining the neurologic consequences of preterm birth. N Engl J Med 2023;389(5):441–53.
[3] Vutskits L. Cerebral blood flow in the neonate. Paediatr Anaesth 2014;24(1):22–9.
[4] Hoffman SB, Cheng YJ, Magder LS, Shet N, Viscardi RM. Cerebral autoregulation in premature infants during the first 96 hours of life and relationship to adverse outcomes. Arch Dis Child Fetal Neonatal Ed 2019;104(5):F473–9.
[5] Sorensen LC, Maroun LL, Borch K, Lou HC, Greisen G. Neonatal cerebral oxygenation is not linked to foetal vasculitis and predicts intraventricular haemorrhage in preterm infants. Acta Paediatr 2008;97(11):1529–34.
[6] Dix LM, van Bel F, Lemmers PM. Monitoring cerebral oxygenation in neonates: an update. Front Pediatr 2017;5:46.
[7] Gibbs V, Cole D, Sassano A. Ultrasound physics and technology: how, why and when. 1st ed Edinburgh: Churchill Livingstone; 2009.
[8] Dudink J, Jeanne Steggerda S, Horsch S. State-of-the-art neonatal cerebral ultrasound: technique and reporting. Pediatr Res 2020;87(Suppl. 1):3–12.
[9] Leijser LM, de Vries LS, Cowan FM. Using cerebral ultrasound effectively in the newborn infant. Early Hum Dev 2006;82(12):827–35.
[10] de Goederen R, Vos HJ, de Jong N, Horsch S, Dudink J. Future applications of advanced neonatal cerebral ultrasound. Paediatr Child Health (Oxford) 2018;28(1):28–33.
[11] Szabo TL. Chapter 11 – Doppler modes. In: Szabo TL, editor. Diagnostic ultrasound imaging: inside out. 2nd ed. Boston: Academic Press; 2014. p. 431–500.
[12] Blankenberg FG, Loh NN, Norbash AM, Craychee JA, Spielman DM, Person BL, et al. Impaired cerebrovascular autoregulation after hypoxic-ischemic injury in extremely low-birth-weight neonates: detection with power and pulsed wave Doppler US. Radiology 1997;205(2):563–8.
[13] Demene C, Pernot M, Biran V, Alison M, Fink M, Baud O, et al. Ultrafast Doppler reveals the mapping of cerebral vascular resistivity in neonates. J Cereb Blood Flow Metab 2014;34(6):1009–17.
[14] Evans DH, Levene MI, Shortland DB, Archer LN. Resistance index, blood flow velocity, and resistance-area product in the cerebral arteries of very low birth weight infants during the first week of life. Ultrasound Med Biol 1988;14(2):103–10.
[15] Camfferman FA, de Goederen R, Govaert P, Dudink J, van Bel F, Pellicer A, et al. Diagnostic and predictive value of Doppler ultrasound for evaluation of the brain circulation in preterm infants: a systematic review. Pediatr Res 2020;87(Suppl. 1):50–8.
[16] Tanter M, Fink M. Ultrafast imaging in biomedical ultrasound. IEEE Trans Ultrason Ferroelectr Freq Control 2014;61(1):102–19.
[17] Mace E, Montaldo G, Osmanski BF, Cohen I, Fink M, Tanter M. Functional ultrasound imaging of the brain: theory and basic principles. IEEE Trans Ultrason Ferroelectr Freq Control 2013;60(3):492–506.
[18] Maresca D, Correia M, Villemain O, Bizé A, Sambin L, Tanter M, et al. Noninvasive imaging of the coronary vasculature using ultrafast ultrasound. JACC Cardiovasc Imaging 2018;11(6):798–808.
[19] Osmanski BF, Pernot M, Montaldo G, Bel A, Messas E, Tanter M. Ultrafast Doppler imaging of blood flow dynamics in the myocardium. IEEE Trans Med Imaging 2012;31(8):1661–8.
[20] Ekroll IK, Dahl T, Torp H, Løvstakken L. Combined vector velocity and spectral Doppler imaging for improved imaging of complex blood flow in the carotid arteries. Ultrasound Med Biol 2014;40(7):1629–40.
[21] Provost J, Papadacci C, Arango JE, Imbault M, Fink M, Gennisson JL, et al. 3D ultrafast ultrasound imaging in vivo. Phys Med Biol 2014;59(19):L1–13.
[22] Urs R, Ketterling JA, Silverman RH. Ultrafast ultrasound imaging of ocular anatomy and blood flow. Invest Ophthalmol Vis Sci 2016;57(8):3810–6.
[23] Baranger J, Demene C, Frerot A, Faure F, Delanoë C, Serroune H, et al. Bedside functional monitoring of the dynamic brain connectivity in human neonates. Nat Commun 2021;12(1):1080.
[24] Fakhari N, Aguet J, Nguyen MB, Zhang N, Mertens L, Jain A, et al. Automated classification of cerebral arteries and veins in the neonate using ultrafast doppler spectrogram. Phys Med Biol 2024;69(24):245006.
[25] Fakhari N, Aguet J, Howell A, Nguyen M, Mertens L, Crawford L, et al. Towards quantitative assessment of cerebrovascular autoregulation in human neonates using ultrafast ultrasound imaging. Sci Rep 2025;15(1):12374.
[26] Dudink J, Lequin M, Weisglas-Kuperus N, Conneman N, van Goudoever JB, Govaert P. Venous subtypes of preterm periventricular haemorrhagic infarction. Arch Dis Child Fetal Neonatal Ed 2008;93(3):F201–6.
[27] Couture O, Hingot V, Heiles B, Muleki-Seya P, Tanter M. Ultrasound localization microscopy and super-resolution: a state of the art. IEEE Trans Ultrason Ferroelectr Freq Control 2018;65(8):1304–20.
[28] Ecury-Goossen GM, Camfferman FA, Leijser LM, Govaert P, Dudink J. State of the art cranial ultrasound imaging in neonates. J Vis Exp 2015(96):e52238. doi: 10.3791/52238.
[29] Kortenbout AJ, Costerus S, Dudink J, de Jong N, de Graaff JC, Vos HJ, et al. Automatic max-likelihood envelope detection algorithm for quantitative high-frame-rate ultrasound for neonatal brain monitoring. Ultrasound Med Biol 2024;50(3):434–44.

[30] Demené C, Deffieux T, Pernot M, Osmanski BF, Biran V, Gennisson JL, et al. Spatiotemporal clutter filtering of ultrafast ultrasound data highly increases Doppler and fUltrasound sensitivity. IEEE Trans Med Imaging 2015;34(11):2271–85.
[31] Yu A, Lovstakken L. Eigen-based clutter filter design for ultrasound color flow imaging: a review. IEEE Trans Ultrason Ferroelectr Freq Control 2010;57(5):1096–111.
[32] Tang J, Postnov DD, Kilic K, Erdener SE, Lee B, Giblin JT, et al. Functional ultrasound speckle decorrelation-based velocimetry of the brain. Adv Sci 2020;7(18):2001044.
[33] Chen H, Mirg S, Gaddale P, Agrawal S, Li M, Nguyen V, et al. Multiparametric brain hemodynamics imaging using a combined ultrafast ultrasound and photoacoustic system. Adv Sci 2024;11(31):2401467.
[34] Raets M, Dudink J, Raybaud C, Ramenghi L, Lequin M, Govaert P. Brain vein disorders in newborn infants. Dev Med Child Neurol 2015;57(3):229–40.
[35] Camfferman FA, Govaert P, Groenendaal F, Vanderhasselt T, Cools F, Dudink J. Internal cerebral vein doppler velocities reflect maturational changes and hemorrhage risk in preterm infants. Am J Neuroradiol 2026;47(6):1672–80.
[36] Camfferman FA, Govaert P, Lequin MH, Groenendaal F, Tataranno M-L, Kizilates U, et al. Toward a broader classification of deep venous cerebral anatomy in extremely preterm infants: a literature-based approach and its relevance to intraventricular hemorrhage. Am J Neuroradiol 2026;47(2):496–502.
[37] Steinsmo Ødegård S, Jarmund AH, Pedersen SA, Govaert P, Dudink J, Nyrnes SA. A scoping review of variations in cerebral Doppler venous waveforms in infants. Neuroimage 2026;328:121766.
[38] Vik SD, Torp H, Follestad T, Støen R, Nyrnes SA. NeoDoppler: new ultrasound technology for continous cerebral circulation monitoring in neonates. Pediatr Res 2020;87(1):95–103.